

THERMODYNAMIC PROPERTIES OF STRONTIUM METANIOPATE SrNb₂O₆

J. Leitner^{1*}, M. Hampl¹, K. Růžička², M. Straka², D. Sedmidubský³ and P. Svoboda⁴

¹Department of Solid State Engineering, Institute of Chemical Technology, Prague, Technická 5, 166 28 Prague 6, Czech Republic

²Department of Physical Chemistry, Institute of Chemical Technology, Prague, Technická 5, 166 28 Prague 6, Czech Republic

³Department of Inorganic Chemistry, Institute of Chemical Technology, Prague, Technická 5, 166 28 Prague 6, Czech Republic

⁴Department of Electronic Structures, Faculty of Mathematics and Physics, Charles University, Ke Karlovu 5, 120 00 Prague 2 Czech Republic

The heat capacity and the enthalpy increments of strontium metaniopate SrNb₂O₆ were measured by the relaxation method (2–276 K), micro DSC calorimetry (260–320 K) and drop calorimetry (723–1472 K). Temperature dependence of the molar heat capacity in the form $C_{pm}=(200.47\pm 5.51)+(0.02937\pm 0.0760)T-(3.4728\pm 0.3115)\cdot 10^6/T^2$ J K⁻¹ mol⁻¹ (298–1500 K) was derived by the least-squares method from the experimental data. Furthermore, the standard molar entropy at 298.15 K $S_m^0(298.15\text{ K})=173.88\pm 0.39$ J K⁻¹ mol⁻¹ was evaluated from the low temperature heat capacity measurements. The standard enthalpy of formation $\Delta_f H^0(298.15\text{ K})=-2826.78$ kJ mol⁻¹ was derived from total energies obtained by full potential LAPW electronic structure calculations within density functional theory.

Keywords: *ab-initio calculations, ceramics, DSC, oxides, specific heat, thermodynamic properties*

Introduction

Strontium niobates are of considerable interest because they are constituents of practically important ternary systems BaO–SrO–Nb₂O₅ and Bi₂O₃–SrO–Nb₂O₅. The solid solution of SrNb₂O₆ and BaNb₂O₆ has found many technological applications such as electro-optic, pyroelectric, and piezoelectric devices. Ternary oxide SrBi₂Nb₂O₉ is one of the most promising candidates for lead-free non-volatile random access memory applications.

Phase relations in the binary system SrO–Nb₂O₅ were investigated by Carruthers and Grasso [1] and more recently by Leshchenko *et al.* [2]. They are some discrepancies in number and stoichiometry of observed mixed oxides but Sr₂Nb₁₀O₂₇, SrNb₂O₆, Sr₂Nb₂O₇ and Sr₅Nb₄O₁₅ phases were observed in both studies. While in the former study some ranges of homogeneity of SrNb₂O₆ was detected, the definite stoichiometry was observed in the later one. Strontium metaniopate, SrNb₂O₆, occurs in various polymorphic forms [3]. At the temperatures below approx. 1600 K the monoclinic form (space group P21/c) is the stable one [2–6]. Above this temperature the monoclinic phase transforms to the tetragonal one with a tungsten bronze structure. The melting point of SrNb₂O₆ is around 1773 K [2, 3].

Thermodynamic assessment of the system SrO–Nb₂O₅ was performed by Yang *et al.* [7] within which thermodynamic functions of above mentioned

oxides were evaluated. They used so called Calphad technique for the assessment and phase equilibrium data according to [1] were considered. They applied the compound energy model [8] for the description of the slightly non-stoichiometric phase SrNb_{2-x}O_{6-2.5x}. For the strictly stoichiometric compound SrNb₂O₆ they evaluated the following values of the enthalpy and entropy of formation from the constituent binary oxide SrO+Nb₂O₅: $\Delta_{f,ox} H=-325.044$ kJ mol⁻¹ and $\Delta_{f,ox} S=-58.65$ J K⁻¹ mol⁻¹. The heat capacity and the enthalpy increments of SrNb₂O₆ have not been measured yet.

In the course of a systematic study of thermochemical properties of complex oxides in the system Bi₂O₃–SrO–Nb₂O₅, we recently measured the heat capacity and the heat content of BiNbO₄ [9], BiNb₅O₁₄ [10] and SrBi₂Nb₂O₉ [11]. The aim of this paper is the measurement of the heat capacity and the enthalpy increments of strontium metaniopate, SrNb₂O₆, in a broad temperature range, the evaluation of the standard molar entropy at 298.15 K and the temperature dependence of C_{pm} above the room temperature, and the first-principle calculation of the heat of formation at 298.15 K.

Experimental

The sample was prepared by conventional solid state reaction from high purity precursors SrCO₃ (99.9%,

* Author for correspondence: Jindrich.Leitner@vscht.cz

Aldrich) and Nb₂O₅ (99.85%, Alfa Aesar). The stoichiometric amount of SrCO₃ and Nb₂O₅ was ground in agate mortar and heated up to 1000°C in platinum crucible in air atmosphere for 120 h. After regrind, the mixture was treated at 1250°C in air for 120 h.

The phase determination was carried out using XRD. X-ray powder diffraction data were collected at room temperature with an X'Pert PRO θ - θ powder diffractometer with parafocusing Bragg-Brentano geometry using CuK α radiation ($\lambda=1.5418$ Å, $U=40$ kV, $I=30$ mA). Data were scanned over the angular range 5–60° (2 θ) with an increment of 0.02° (2 θ) and a counting time of 0.3 s step⁻¹. Data evaluation was performed by means of the software package HighScore Plus.

An ARL 9400 XP sequential WD-XRF spectrometer was used to perform XRF analysis. It is equipped with an Rh anode end-window X-ray tube type 4GN fitted with 75 μ m Be window. All peak intensity data were collected by software WinXRF in vacuum. The generator settings-collimator-crystal-detector combinations were optimised for all 79 measured elements with an analysis time of 6 s per element. The obtained data were evaluated by the software UniQuant 4 operating without using standards. The analysed powders were pressed into pellets about 5 mm thick and diameter of 40 mm without any binding agent and covered with 4 μ m supporting polypropylene (PP) film. The time of measurement was about 15 min.

The PPMS equipment (Quantum Design) was used for the heat capacity measurements in the low-temperature region. The samples for heat-capacity measurements in the PPMS apparatus were in a form of compressed powder plates of typical mass of about 15 mg. The density of the pressed sample was 70.6% of the theoretical one. The sample was mounted to the calorimeter platform using standard cryogenic grease Apiezon N. The procedure was as follows: first, a blank sample holder with the Apiezon only was measured in the temperature range 2–300 K to get the background data, then the sample plate was attached to the calorimeter platform using the Apiezon as an adhesive and the measurement was repeated in the same temperature range with the same temperature steps. The sample specific heat was then obtained as a difference of the two data sets. This procedure was applied, since the specific heat of Apiezon is not negligible in comparison with the specific heat of the sample (~8% at the room temperature) and exhibits a sol-gel transition below the room temperature [12].

The heat capacity measurements in the PPMS were performed by the relaxation method [13] with fully automatic procedure under high vacuum (pressure $\sim 10^{-2}$ Pa) to avoid the heat loss through the exchange gas. The manufacturer claims the precision of this measurement better than 2% [14], the control

measurement of the copper sample (99.999% purity) confirmed this precision. On the other hand, the precision of the measurement strongly depends on the thermal coupling between the sample and the calorimeter platform. Due to unavoidable porosity of the sample plate this coupling is rapidly worsening at temperatures ~ 270 K and higher as the Apiezon diffuses into the porous sample. Because of that, only the data up to 275 K were considered as reliable and used for the calculation.

The Micro DSC III calorimeter (Setaram) was used for the heat capacity determination in the temperature range of 260–352 K. The measurements were carried out in the incremental temperature scanning mode with a number of 5–10 K steps (heating rate 0.2 K min⁻¹) followed by isothermal delays of 9000 s. The synthetic sapphire, NIST Standard reference material No. 720, was used as the reference material. The typical mass of samples was ~ 0.4 g. The uncertainty of heat capacity measurements is estimated to be better than $\pm 1\%$.

Enthalpy increment determinations were carried out by drop method using the high temperature calorimeter Multi HTC 96 (Setaram). All measurements were performed in air by alternating dropping of the reference material (small pieces of synthetic sapphire, NIST Standard reference material No. 720) and of the sample (SrNb₂O₆ pellets, 5 mm in diameter, thickness of 1–2 mm) being initially held at room temperature (T_0) through a lock into the working cell of the pre-heated calorimeter. Endothermic effects are detected and the relevant peak area is proportional to the heat content of the dropped specimen. The measurements were performed at temperatures 723–1472 K on samples with the masses 100–200 mg. The delays between two subsequent drops were 40–50 min. In order to check for the accuracy of the present measurement, the heat content of platinum was measured first and compared with published values [15–17]. Estimated overall accuracy of the drop measurements is $\pm 3\%$.

First principle calculation

The ab-initio calculations based on density functional theory represent an alternative method to various experimental techniques to assess the enthalpies of formation of stoichiometric compounds. Among them, the full potential LAPW method combined with general gradient approximation (GGA) to treat the exchange-correlation potential has proven to yield the most accurate results of total energies. In the present study, we employed its modified version, APW+lo, as implemented in WIEN2k code [18]. In order to obtain the ground state ($T=0$ K) enthalpy of formation, $\Delta_f H^0$ (0 K), the total energies of solid Sr and Nb, and gaseous

O₂ have to be subtracted from the total energy of SrNb₂O₆. Since the calculation of an isolated O₂ molecule yielding a reliable energy value is a relatively difficult task by means of LAPW, we preferred to perform the calculations for SrO and Sr, and to take use of the assessed value of $\Delta_f H^0$ (SrO, 298.15 K) = -592.15 kJ mol⁻¹ [19]. The refined lattice parameters given below were used in the calculation of SrNb₂O₆, whereas those of Sr, SrO, Nb were minimized with respect to calculated total energy, getting the values close to experimental ones [20]. All calculations were performed with a *k*-mesh of 2000 points per first Brillouin zone and the parameter $R_{MT}K_{max}=8.0$, where K_{max} is the cut-off for plane wave expansion and $R_{MT}=0.321$ nm is the smallest of the selected muffin-tin radii, $R_{MT}(Sr)=0.378$ nm, $R_{MT}(Nb)=0.340$ nm, $R_{MT}(O)=0.321$ nm.

Results and discussion

The XRD analysis (Fig. 1) revealed that the prepared samples consist of single phase with monoclinic structure without any observable diffraction lines from unreacted precursors or other phases. The following lattice parameters of the prepared samples were evaluated by Rietveld refinement using published atomic positions [20]: $a=0.772085\pm0.000029$ nm, $b=0.559303\pm0.000023$ nm, $c=1.09821\pm0.000040$ nm and $\beta=90.3739\pm0.0025$. They are in excellent agreement with the values published recently [2–6].

Based on the X-ray fluorescence spectroscopy, the composition of our sample is: (27.38±0.22) mass% SrO and (72.54±0.22) mass% Nb₂O₅. This corresponds to stoichiometric formula Sr_{0.97}Nb_{2.00}O_{5.97}. The oxygen stoichiometry was not determined but calculated with respect to the valence of metal ions Sr²⁺ and Nb⁵⁺. Calcium oxide was detected as the most abundant impurity: (0.04±0.01) mass% CaO.

The measured C_{pm} data involving 216 points (2 runs) from relaxation time and 26 points (3 runs) from micro DSC are plotted in Fig. 2. The enthalpy

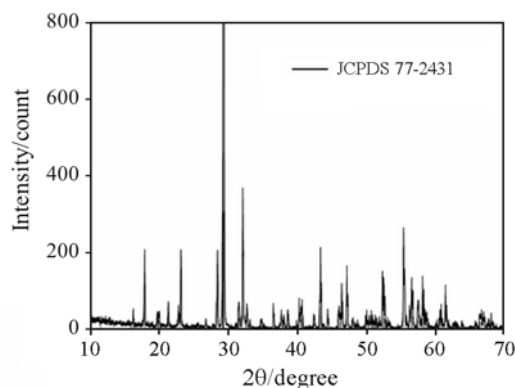


Fig. 1 X-ray diffraction pattern of SrNb₂O₆

increment data (28 points) are listed in Table 1 and shown in Fig. 3.

The raw data were analyzed in two separate steps. The low-temperature part of the heat capacity has been described as a sum of electronic and phonon parts, respectively. The electronic part of the specific heat was then described by a standard Sommerfeld linear approximation $C_{pm,el}=\gamma_{el}T$, which yields the value of the Sommerfeld coefficient $\gamma_{el}=6\cdot 10^{-4}$ J K⁻² mol⁻¹. This is a reasonable value considering the insulating character of the studied material. The analysis of the phonon specific heat was performed as an additive combination of Debye and Einstein models. The phonon spectrum of a polyatomic compound contains three acoustic branches and $3n-3$ optical ones, where n is number of atoms per formula unit. In our case, i.e. 9 atoms/f.u., this represents 24 optical branches. Let us note that this approach is still a simplification, since n should properly refer to the number of atoms per primitive unit cell containing, in this instance, four formula units. However, this would lead to an inadequate increase of parameters to be fitted. Both models include corrections for anharmonicity, which is responsible for small, but not negligible additive term at higher temperatures and which accounts for the discrepancy between isobaric and isochoric specific heat. This correction factor is considered in the form $1/(1-\alpha T)$, according to [21].

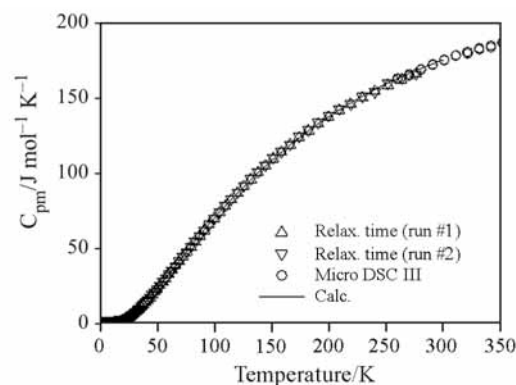


Fig. 2 Heat capacity of SrNb₂O₆

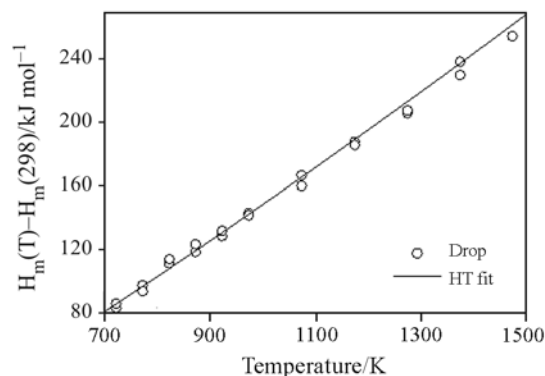


Fig. 3 Heat content of SrNb₂O₆

Table 1 Enthalpy increments of strontium metaniobate SrNb₂O₆

<i>T</i> /K	$H_m(T)-H_m(298.15)/\text{J mol}^{-1}$ experimental	$H_m(T)-H_m(298.15)/\text{J mol}^{-1}$ integration of Eq. (1)	$\delta/\%$ [#]
722.7	84018	86272	2.7
722.8	86570	86276	-0.3
772.8	98038	97281	-0.7
772.8	94329	97292	3.2
822.9	111960	108420	-3.1
823.5	114535	108561	-5.2
872.9	119019	119647	0.5
872.9	123838	119649	-3.4
922.9	129024	130980	1.5
922.9	132254	130987	-0.9
973.3	143318	142478	-0.6
973.3	141943	142490	0.4
1023.2	158660	153990	-2.9
1023.2	155666	153990	-1.1
1073.4	166851	165635	-0.7
1073.5	160329	165656	3.3
1123.3	178491	177299	-0.7
1123.3	178031	177311	-0.4
1173.7	187786	189168	0.7
1173.7	185855	189177	1.8
1223.4	201241	200963	-0.1
1273.4	205843	212926	3.4
1273.4	207390	212931	2.7
1322.7	229156	224788	-1.9
1322.8	228449	224805	-1.6
1372.9	238064	236954	-0.5
1372.9	229759	236957	3.1
1471.9	254116	261182	2.7

$\delta=100(\text{calc.}-\text{exp.})/\text{exp}$

The acoustic part of the phonon specific heat is then described using the Debye model in the form

$$C_{\text{phD}} = \frac{9T}{1 - \alpha_D T} \left(\frac{T}{\Theta_D} \right)^3 \int_0^{x_D} \frac{x^4 \exp(x)}{[\exp(x) - 1]^2} dx \quad (1)$$

where R is the gas constant, Θ_D is the Debye characteristic temperature, α_D is the coefficient of anharmonicity of acoustic branches and $x_D = \Theta_D/T$. Here the three acoustic branches are taken as one triply degenerate branch. Similarly, the individual optical branches are described by the Einstein model

$$C_{\text{phEi}} = \frac{R}{1 - \alpha_{\text{Ei}} T} x_{\text{Ei}}^2 \frac{\exp x_{\text{Ei}}}{(\exp x_{\text{Ei}} - 1)^2} \quad (2)$$

where α_{Ei} and x_{Ei} have analogous meanings as in the previous case. To reduce number of adjustable param-

eters, several optical branches are again grouped into one degenerate multiple branch with the same Einstein characteristic temperature and anharmonicity coefficient, respectively. This way we have succeeded to describe the 24 optical branches in terms of five Einstein modes with the respective degeneracies 2-6-6-8-2. The analysis of the phonon specific heat is summarized in Table 2. The description of the phonon specific heat is then taken as

$$C_{\text{ph}} = C_{\text{phD}} + \sum_{i=1}^{3n-3} C_{\text{phEi}} \quad (3)$$

For the assessment of C_{pm} function above room temperature, the heat capacity data from Micro DSC and the enthalpy increment data from drop calorimetry were treated simultaneously. Different masses w_i were assigned to individual points calculated as $w_i =$

Table 2 Parameters for the phonon specific heat

Type	Degeneracy	Characteristic temp./K	Anharmonicity coeff./10 ⁻⁵ K ⁻¹
Acoustic	3	241±1	5±1
	2	139±1	8±1.5
	6	312±2	5±1
Optical	6	444±2	6±1
	8	824±5	3±0.8
	2	956±5	1±0.5

1/δ_i² where δ_i is absolute deviation of the *i*th measurement estimated from overall accuracies of the measurements (1% for Micro DSC and 3% for drop calorimetry). Both types of experimental data thus gain comparable significance during the regression analysis. The temperature dependence of the molar heat capacity of solid SrNb₂O₆ can thus be expressed by (*T*=298.15–1500 K):

$$C_{pm} = (200.47 \pm 5.51) + (0.02937 \pm 0.0760)T - \frac{(3.4728 \pm 0.3115) \cdot 10^6}{T^2} \text{ (J K}^{-1} \text{ mol}^{-1}) \quad (4)$$

The heat capacity as a function of temperature according to Eq. (4) is shown in Fig. 4. The dependence calculated according to the empirical Neumann–Kopp's rule [22] is given there for comparison.

The value of standard molar entropy of SrNb₂O₆ at 298.15 K $S_m^0(298.15 \text{ K}) = 173.88 \pm 0.39 \text{ J mol}^{-1} \text{ K}^{-1}$ was derived from the low-temperature C_{pm} data by integrating the C_{pm}/T functions from zero to 298.15 K. A numerical integration (the trapezoid rule) was used with the boundary conditions $S_m^0(0 \text{ K}) = 0$ and $C_{pm}/T = 0$ for $T = 0 \text{ K}$. Standard deviations (2σ) were calculated using the error propagation law. This value as well as the standard entropy of formation from the constituent binary oxides, $\Delta_{f,ox}S$, are listed in Table 3

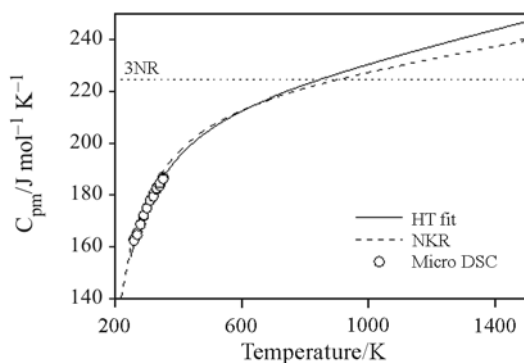


Fig. 4 Temperature dependence of the heat capacity of SrNb₂O₆ calculated according to Eq. (4) and according to the Neumann–Kopp's additive rules. Dotted line represents the Dulong–Petit limit

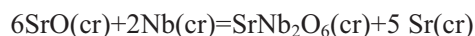
Table 3 Standard molar entropies and standard entropies of formation from the constituent binary oxides of mixed oxides in the system SrO–Bi₂O₃–Nb₂O₅

Oxide	$S_m^0(298.15 \text{ K}) / \text{J K}^{-1} \text{ mol}^{-1}$	$\Delta_{f,ox}S(298.15 \text{ K}) / \text{J K}^{-1} \text{ mol}^{-1}$
SrO	53.58 [19]	
Bi ₂ O ₃	148.5 [23]	
Nb ₂ O ₅	137.30 [24]	
SrNb ₂ O ₆	173.88±0.39 ^a	-17.00
Sr ₂ Nb ₂ O ₇	232.37 ^b	-12.09
SrNb ₂ O ₆		-58.65 ^c
Sr ₂ Nb ₂ O ₇		-39.93 ^c
Sr ₂ Nb ₁₀ O ₂₇		-350.69 ^c
Sr ₃ Nb ₄ O ₁₅		-51.01 ^c
SrBi ₂ O ₄		-12 ^d
Sr ₂ Bi ₂ O ₅		-24 ^d
Sr ₃ Bi ₂ O ₆		-7 ^d
BiNbO ₄	147.86 ^e	4.96
BiNb ₅ O ₁₄	397.17 ^f	-25.82
SrBi ₂ Nb ₂ O ₉	327.15±0.80 ^g	-12.23

^aThis work, ^bbased on low-temperature calorimetric data [25], ^cthermodynamic assessment [7], ^dthermodynamic assessment [26], ^ebased on low-temperature calorimetric data [9], ^fbased on low-temperature calorimetric data [10], ^gbased on low-temperature calorimetric data [11]

together with the values of $\Delta_{f,ox}S$ for other mixed oxides in the system SrO–Bi₂O₃–Nb₂O₅.

As noted above, the total energy of gaseous O₂ needed to evaluate the enthalpy of formation was not calculated directly in WIEN2k, but derived from the corresponding values of calculated total energies of SrO and Sr and the experimental value of $\Delta_f H^0(298.15 \text{ K})$ for SrO. Hence, the formal reaction, from which the resulting enthalpy of formation was directly derived, reads



In order to recalculate the data from the temperature of reference state $T = 298.15 \text{ K}$ to the ground state temperature $T = 0 \text{ K}$, which the LAPW calculations are referred to, and vice-versa, the value of $H_m(298.15) - H_m(0) = 28.722 \text{ kJ mol}^{-1}$ derived from the measured low temperature C_{pm} of SrNb₂O₆ as well as the literature data for SrO, Sr, Nb and O₂ [26] were used. The standard enthalpy of formation $\Delta_f H^0(298.15 \text{ K}) = -2826.78 \text{ kJ mol}^{-1}$ was hereby obtained. The corresponding enthalpy of formation from the constituent oxides, SrO and Nb₂O₅ at 298.15 K is $\Delta_{f,ox}H^0(298.15 \text{ K}) = -335.20 \text{ kJ mol}^{-1}$.

While the value of $\Delta_{f,ox}H^0(298.15 \text{ K})$ based on ab-initio calculation and that derived from the equilibrium with a high temperature liquid phase [7] agree very

well, there is a large difference between the value of $\Delta_{f,ox}S^0(298.15\text{ K})$ derived from low-temperature C_{pm} data and the assessment result [7]. The value of standard molar entropy $S_m^0(298.15\text{ K})=132.23\text{ J K}^{-1}\text{ mol}^{-1}$ based on the phase diagram data optimization [7] is unexpectedly low. The same applies for $\text{Sr}_2\text{Nb}_2\text{O}_7$ for which the assessed value $S_m^0(298.15\text{ K})=204.53\text{ J K}^{-1}\text{ mol}^{-1}$ [7] is significantly lower than the calorimetric value $S_m^0(298.15)=232.37\text{ J K}^{-1}\text{ mol}^{-1}$ [25]. For that reason we consider the value $S_m^0(298.15\text{ K})=173.88\text{ J K}^{-1}\text{ mol}^{-1}$ derived in this work as a more reliable.

Using our data it is possible to calculate the standard molar Gibbs energy of solid SrNb_2O_6 at the temperature of its fusion $T=1773\text{ K}$ [1, 2]: $G_m^0(\text{SrNb}_2\text{O}_6,cr,1773\text{ K})=-3481.062\text{ kJ mol}^{-1}$. On the other hand Gibbs energy of a stoichiometric liquid $(\text{SrO}+\text{Nb}_2\text{O}_3)(l)$ at 1773 K can be calculated using model parameters given by Yang *et al.*, [7]: $G(l,1773\text{ K})=-3411.895\text{ kJ}$. The difference of 69.167 kJ implies that the model parameters for liquid have to be reassessed.

Acknowledgements

This work was supported by the Ministry of Education of the Czech Republic (Research Projects Nos MSM6046137302 and MSM6046137307). The work of P. S. is a part of the research program MSM0021620834 financed by the Ministry of Education of the Czech Republic.

References

- J. R. Carruthers and M. Grasso, *J. Electrochem. Soc.*, 117 (1970) 1426.
- P. P. Leshchenko, A. V. Shevchenko, L. N. Lykova, L. M. Kovba and E. A. Ippolitova, *Izv. Akad. Nauk SSSR, Neorg. Mater.*, 18 (1982) 1202.
- K. L. Keester, R. R. Neurgaonkar, T. C. Lim and E. J. Staples, *Mater. Res. Bull.*, 15 (1980) 821.
- V. K. Trunov, I. M. Averina and Yu. A. Velikodnyi, *Kristallografiya*, 26 (1981) 390.
- B. O. Marinder P. Wang, W. Ling and E. Per, *Acta Chem. Scand.*, A40 (1986) 467.
- V. P. Sirovinkin and S. P. Sirovinkin, *Zh. Neorg. Khim.*, 38 (1993) 1071.
- Y. Yang, H. Yu and Z. Jin, *J. Mater. Sci. Technol.*, 15 (1999) 203.
- M. Hillert, B. Jansson and B. Sundman, *Z. Metallkd.*, 79 (1988) 81.
- M. Hampl, A. Strejc, D. Sedmidubský, K. Růžička, J. Hejtmánek and J. Leitner, *J. Solid State Chem.*, 179 (2006) 77.
- M. Hampl, J. Leitner, K. Růžička, M. Straka and P. Svoboda, *J. Therm. Anal. Cal.*, 87 (2007) 553.
- J. Leitner, M. Hampl, K. Růžička, D. Sedmidubský, P. Svoboda and J. Vejpravová, *Thermochim. Acta*, 450 (2006) 105.
- W. Schnelle, J. Engelhardt and E. Gmelin, *Cryogenics*, 39 (1999) 271.
- J. S. Hwang, K. T. Lin and C. Tien, *Rev. Sci. Instrum.*, 68 (1997) 94.
- Quantum Design, Physical Property Measurement System – Application Note, <http://qdusa.com/pdf/brochures/heat.pdf>.
- A. T. Dinsdale, *CALPHAD*, 15 (1991) 317.
- J. W. Arblaster, *Platinum Metals Rev.*, 38 (1994) 119.
- B. Wilthan, C. Cagran, C. Brunner and G. Pottlacher, *Thermochim. Acta*, 415 (2004) 47.
- P. Blaha, K. Schwarz, G. Madsen, D. Kvasnicka and J. Luitz, *WIEN2k, An Augmented Plane Wave+Local Orbitals Program for Calculating Crystal Properties*, Techn. Universität Wien, Austria 2002.
- D. Risold, B. Hallstedt and L. J. Gauckler, *CALPHAD*, 20 (1996) 353.
- Inorganic Crystal Structure Database, ver. 1.3.3., FIZ Karlsruhe - NIST Gaithersburg 2004.
- C. A. Martin, *J. Phys.: Condens. Matter*, 3 (1991) 5967.
- J. Leitner, P. Chuchvalec D. Sedmidubský, A. Strejc and P. Abrman, *Thermochim. Acta*, 395 (2003) 25.
- D. Risold, B. Hallstedt, L. J. Gauckler, H. L. Lukas and S. G. Fries, *J. Phase Equilib.*, 16 (1995) 223.
- O. Knacke, O. Kubaschewski and K. Hesselmann, *Thermochemical Properties of Inorganic Substances*, 2nd Ed., Springer, Berlin 1991.
- Y. Akishige, H. Shigematsu, T. Tojo, H. Kawaji and T. Atake, *J. Therm. Anal. Cal.*, 81 (2005) 537.
- B. Hallstedt, D. Risold and L. J. Gauckler, *J. Am. Ceram. Soc.*, 80 (1997) 1085.
- M. W. Chase, Jr. (Ed.), *NIST-JANAF Thermochemical Tables*, 4th Ed., *J. Phys. Chem. Ref. Data*, Monograph No. 9, ASC-AIP-NSRDS, New York 1998.

Received: June 6, 2007

Accepted: June 11, 2007

DOI: 10.1007/s10973-007-8592-8